Scientific paper

### One-Step Synthesis of Biocompatible Thiosemicarbazone Functionalized Copper Oxide Nanoparticles: Evaluation of Enhanced Antibacterial Activity

Seyede Khadije Safavi-Mirmahaleh, <sup>1</sup> Zeinab Moradi-Shoeili<sup>0</sup>, <sup>1,\*</sup> and Mehdi Rassa<sup>2</sup>

<sup>1</sup> Department of Chemistry, Faculty of Sciences, University of Guilan, P.O. Box 41335-1914, Rasht, Iran

<sup>2</sup> Department of Biology, Faculty of Sciences, University of Guilan, P.O. Box 41335–1914, Rasht, Iran

\* Corresponding author: E-mail: zmoradi@guilan.ac.ir Tel.: +98 13 33333262; fax: +98 13 33320066

Received: 02-13-2023

#### **Abstract**

Organic–inorganic hybrid bioactive nanomaterials were sonochemically synthesized by covalent anchoring of 2-acetylpyridine thiosemicarbazone on the surface of CuO nanoparticles using two different approaches. The prepared nanoparticles were characterized by a combination of physico-chemical and spectroscopic techniques. The synergetic bactericidal activity of CuO and thiosemicarbazone moieties in prepared nanomaterials was tested *in vitro* using the zone inhibition methods against Gram positive and Gram negative bacterial strains. Additionally, the minimum inhibitory concentration (MIC) and minimal bactericidal concentration (MBC) were also determined. Results prove that CuO and functionalized CuO nanoparticles synthesized by the sonochemical method in present study show improved antibacterial activities and they could be used in the design of more efficient antibacterial materials for pharmaceutical applications.

Keywords: Copper oxide; Thiosemicarbazone, Nanoparticles; Antibacterial activity.

#### 1. Introduction

In recent years, the need to develop novel drugs with enhanced, targeted bactericidal activity has significantly increased due to concerns regarding drug-resistance in pathogens. With recent advances in nanotechnology, nano-sized materials have received considerable attention as potent antimicrobial agents because of their unusual properties which are distinctly different from those of their micrometer-sized counterparts.<sup>2-4</sup> As antimicrobial agents, nanomaterials show a diversity of modes of action; such as electrostatic interaction with the bacterial membrane, reactive oxygen species (ROS) production, photoactivation or photocatalism, production of reactive nitrogen species (RNS), production and induction of signal secretion, which may cause membrane damage, hinder protein function, induce DNA destruction and therefore promote apoptosis (programmed cell death).5

For more than a decade, various types of metals such as silver (Ag)<sup>6</sup> and gold (Au)<sup>7</sup> and also metal oxide nanoparticles such as iron oxide (Fe<sub>3</sub>O<sub>4</sub>),<sup>8</sup> titanium oxide

 $(TiO_2)$ , magnesium oxides (MgO), aluminum oxide  $(Al_2O_3)$ , and zinc oxide  $(ZnO)^{12}$  have been the focus of intense research due to their antimicrobial properties. Moreover, copper oxide (CuO) is among a group of metallo-drugs which can act as effective antimicrobial and antibacterial agents. The higher antibacterial activity of CuO nanoparticles compared to metal nanoparticles such as silver can be interpreted by the stronger complexation of amine and carboxyl groups on the bacterial cell walls and CuO nanoparticles.

The antimicrobial activity of nanomaterials has been observed to vary as a function of environmental factors including pH, temperature, and solvent as well as size, shape, surface area in contact with the microbe, and composition with other organic or inorganic materials. <sup>15–18</sup> In addition, it has been shown that surface chemical modification can improve colloidal stability in physiological media, water solubility, biocompatibility, and specific targeting ability of nanopartricles. <sup>19</sup> After the first report of pyridine-2-carbaldehyde thiosemicarbazone synthesis and its carcinostatic properties, <sup>20</sup> the synthesis of different thiosemicarbazone ligands

and their metal complexes have received considerable attention due to the wide range of applications in pharmacological fields.<sup>21,22</sup> Taking into consideration the advanced applications of nanocomposite materials in the field of antimicrobial chemotherapy, the present work reports a simple and cost effective method for conjugation of bioactive 2-acetylpyridine thiosemicarbazone (TSCPy) on the surface of CuO nanoparticles. CuO nanoparticles containing TSCPy moiety were prepared via two different methods using ultrasonic irradiations. The first route (method A) involves the co-precipitation method in the presence of glutamic acid as conjugating agents. The TSCPy molecules were then anchored on the surface of CuO nanoparticles by a condensation reaction between glutamic acid and TSCPv. In the second route (method B), the TSCPy functionalized CuO nanoparticles were directly synthesized by the co-precipitation method in the presence of TSCPy. The prepared factionalized CuO nanoparticles were characterized by different spectroscopic methods. In addition, the synergetic in vitro antibacterial activity of CuO nanoparticles and TSCPy moiety have been screened against a series of Gram positive and Gram negative bacteria, using the zone inhibition method. The minimum inhibitory concentration (MIC) and minimal bactericidal concentration (MBC) were also investigated.

#### 2. Experimental

#### 2. 1. Materials and Methods

All reagents were obtained from commercial sources and used without further purification. Powder X-ray diffraction (PXRD) data were collected with a Philips pw 1830 diffractometer (Cu-K $\alpha$  X-radiation,  $\lambda$  = 1.54 Å). FT-IR spectra of samples in the form of KBr pellets were recorded using an Alpha-Bruker FT-IR spectrophotometer. The scanning electron microscopy (SEM) images were taken on a KYKY-EM3200 scanning electron microscope. The elemental analysis was recorded with an energy dispersive X-ray (EDX) analyzer, MIRA3 FEG-SEM series.

# 2. 2. Preparation of (E)-2-(1-(pyridin-2-yl) ethylidene)hydrazine-1-carbothioamide (TSCPy)

2-acetylpyridine (0.121 mL, 1 mmol) was added to 20 mL ethanolic solution of the thiosemicarbazide (0.203 g, 1 mmol). The reaction mixture was refluxed for 10 h at 70 °C. A precipitate was formed when the solution was allowed to cool at room temperature. The pale yellow precipitate was filtered, washed with cold ethanol, diethyl ether and dried in air.

#### 2. 3. Preparation of CuO Nanoparticles

Aqueous solution of NaOH (1 M) was added dropwise to 50 mL aqueous solution of CuSO<sub>4</sub>·5H<sub>2</sub>O (6.24 g, 25

mmol) while it was positioned in a large-density ultrasonic probe, operating at 37 kHz with a maximum force output of 320 W (pH 11–12). A black precipitate was formed, and the suspension was then sonicated for 2 h at 30 °C to ensure completion of the reaction. The product was separated by centrifugation, washed with distilled water, ethanol and diethyl ether and dried in air.

### 2. 4. Preparation of Functionalized CuO Nanoparticles

To prepare functionalized CuO nanoparticles with glutamic acid (CuOGA NPs), glutamic acid (0.92 g, 6 mmol) was dissolved in 15 mL of NaOH solution (0.02 M) and then added to an aqueous solution of  $\text{CuSO}_4\text{-}5\text{H}_2\text{O}$  (1.56 g, 6 mmol). The rest of the reaction was carried out according to the procedure described above for CuO nanoparticles. To conjugate CuOGA NPs with TSCPy, 0.3 g of CuOGA was added to 30 mL ethanol and sonicated for 30 min. Then, 0.3 g of TSCPy was dissolved in DMSO (0.1 mL) and 10 mL ethanol was added to the ethanolic suspension of CuOGA. The mixture was sonicated for 60 min and allowed to stir overnight at 40 °C. CuOGA-TSCPy NPs were subsequently washed with ethanol and diethyl ether and dried in oven at 70 °C for 3 h.

The synthesis of TSCPy functionalized CuO nanoparticles (CuOTSCPy) were performed following the procedure described for CuOGA, except that TSCPy (1.05 g, 4 mmol) was used as the functionalization agent.

#### 2. 5. *In-vitro* Antibacterial Assay

Antibacterial activity of the prepared CuO and functionalized CuO NPs were tested in vitro using the zone inhibition method<sup>23</sup> against two Gram positive bacterial strains Micrococcus luteus (ATCC 4698) and Staphylococcus aureus (ATCC 29213), and two Gram negative bacterial strains Escherichia coli (ATCC 25922) and Pseudomonas aeruginosa (ATCC 27853). The nutrient agar and nutrient broth cultures were prepared according to manufactures' instructions and were incubated at 37 °C. After incubation for the appropriate time, a suspension of 50 µL of each bacterial test organism was spread onto the nutrient agar plates. Agar wells were prepared with the help of a sterilized glass tube. Then 30 µL of the test agents at a concentration of 2000 µg/ml in DMSO were added to each well. All the bacterial strains were incubated at 37 °C for 24 h. Clear zones around the wells showed inhibition of bacterial growth and turbidity indicated bacterial resistance to the compound at the concentration present in the medium. The diameter of inhibition zones was determined in millimeters (mm). The concentration of DMSO in the medium did not affect growth of any of the microorganisms tested. All experiments were carried out in triplicate. The results are reported as mean±standard deviation of zone of inhibition in millimeter. Antibacterial activity of each

compound was compared with penicillin G and tetracycline as standard drugs. DMSO was used as a negative control. The MIC and MBC were also determined by the dilution method against the tested bacterial species. The MIC is defined as the lowest concentration of compound that inhibited bacterial growth (no turbidity in the tube). Briefly, NPs were diluted into concentrations of 20, 10, 5 and 2.5 µg/ml, in nutrient broth tubes inoculated with the test bacterium. The tubes were incubated at 37 °C for 24 h and thereafter observed for growth or turbidity using unaided eye. The MBC was defined as the lowest concentration of compound lethal to the bacteria. In brief, 50 µL of broth from each test tube showing no visible signs of growth/ turbidity, was inoculated onto a nutrient agar plate and incubated further for 24 h at 37 °C. The agar plates were then examined for growth.

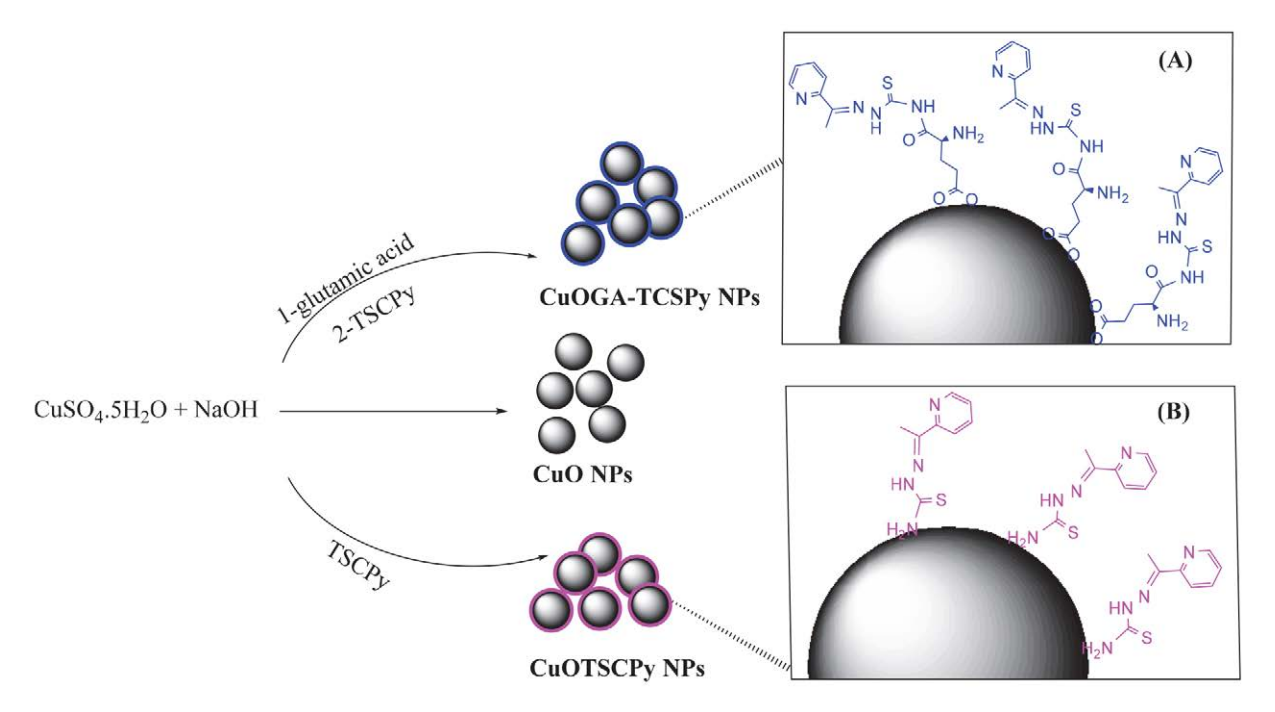
#### 3. Result and Discussion

## 3. 1. Preparation and Characterization of Spinel Ferrite Nanoparticles

The thiosemicarbazone ligand (TSCPy) derived from 2-acetopyridine and thiosemicarbazid was synthesized following the procedure described previously. <sup>24</sup> CuO and also functionalized CuO nanoparticles were synthesized using ultrasonic irradiations which significantly reduced the synthesis time and temperature. CuO nanoparticles containing the TSCPy bioactive molecule were prepared by using one of two methods shown in Scheme 1. The first route (method **A**) involves the synthesis of CuO

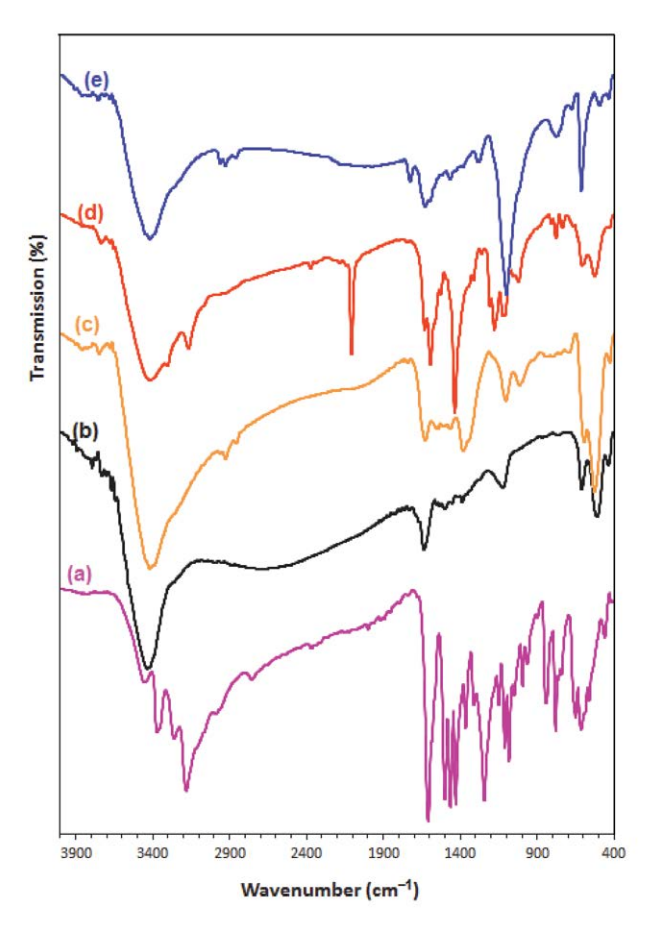
nanoparticles by the co-precipitation method in the presence of glutamic acid. The covalently grafted TSCPy molecules can then be produced via the subsequent condensation reaction between glutamic acid and TSCPy. In the second route (method **B**), the TSCPy functionalized CuO nanoparticles were directly synthesized by the co-precipitation method in the presence of TSCPy.

Figure 1 displays the FT-IR spectra of as-prepared samples. Strong bands around 3460 and 1650 cm<sup>-1</sup> appeared in FT-IR spectra of nano-samples (Figures 1b-1e) corresponding to the vibrational modes of O-H stretching and bending vibrations of surface hydroxyl groups and physisorbed water molecules.<sup>25</sup> FT-IR spectrum for untreated CuO nanoparticles (Figure 1b) displayed strong peaks at 473 cm<sup>-1</sup>, 526 cm<sup>-1</sup> and 618 cm<sup>-1</sup>, which are associated with Cu-O vibrational modes. This is in good agreement with literature sources.<sup>26,27</sup> Glutamic acid and thiosemicarbazone-treated CuO nanoparticles (Figures 1c-1e), in addition to the same two characteristic peaks present in the untreated sample, also showed additional ones. The new bands at about 2850-3050 cm<sup>-1</sup> in CuOGA and CuOGA-TSCPy spectra can be attributed to -C-H bond stretching assigned to the alkyl group.<sup>28</sup> The peaks at 1113 and 1030 cm<sup>-1</sup> in CuOGA spectrum as well as the peaks at 1062 and 1031 cm<sup>-1</sup> in CuOGA-TSCPy spectrum are assigned to C-O stretching coordinated to the metal cations. 14 A comparison between FT-IR spectra of thiosemicarbazone ligand (Figure 1a) and synthesized CuO-GA-TSCPv nanoparticles (Figure 1d) indicates the successful grafting of thiosemicarbazone onto the surface of CuO nanoparticles. The bands at around 3300 cm<sup>-1</sup> and 820 cm<sup>-1</sup> in the IR spectrum of TSCPy corresponding to



Scheme 1. Synthetic pathways for the synthesis of CuO and TSCPy functionalized CuO nanoparticles.

the v(NH) and v(C=S), <sup>29–31</sup> respectively (Figure 1a), have also been observed in IR spectrum of CuOGA-TSCPy nanoparticles (Figure 1d). The band observed at 1210 cm<sup>-1</sup> and a band at 1556 cm<sup>-1</sup> in the spectrum of CuOGA-TSCPy can be assigned to the v(C-N), 32 indicating the thiosemicarbazone anchoring on the CuOGA-TSCPv nanoparticles via amide linkage between glutamic acid and TSCPy. The FT-IR spectra of CuOGA-TSCPy and CuOTSCPy nanoparticles are very similar. Both exhibit the characteristic CuO peaks as well as peaks at around 817 cm<sup>-1</sup> and 3300 cm<sup>-1</sup> corresponding to C=S and N-H bonds, respectively. Furthermore, in the TSCPy treated sample (Figure 1e) multiple C-H stretching peaks above and below 3000 cm<sup>-1</sup> were observed, indicative of both saturated and unsaturated C-H bond stretching. The aromatic C=C stretching peaks including the pyridine skeleton stretching were observed at about 1440 cm<sup>-1</sup> for CuOGA-TSCPv and CuOTSCPy nanoparticles.<sup>33</sup>



**Figure 1.** FT–IR spectra of (a) TSCPy, (b) CuO, (c) CuOGA, (d) CuOGA-TSCPy and (e) CuOTSCPy.

Typical XRD pattern of the synthesized CuO and functionalized CuO nanoparticles are shown in Figure 2. The peaks are indexed as 32.3° (110), 35. 5° (11), 38.7° (111), 49.1° (20), 53.7° (020), 58.2° (202), 61.7° (11), 66.5° (31), 68. 3° (220), 72.6° (311) and 75.5 (004), respectively.

These were compared with the Joint Committee on Powder Diffraction Standards (JCPDS) card No 48–1548. They suggest a monoclinic structure and the diffraction patterns of the characteristic peaks are in good agreement with data presented previously.<sup>34</sup> High intensity and sharpness of CuO XRD characteristic peaks indicate the good quality crystalline structure of nanoparticles. Despite a decrease in intensity observed for the CuOGA-TSCPy sample, it is clear from Figure 2b that the functionalization does not influence the crystal structure. Further, no noticeable peaks such as Cu(OH)<sub>2</sub>, CuS or other copper compound were observed in CuO and CuOGA-TSCPy XRD patterns, indicating the formation of single-phase CuO with a monoclinic structure.

The size of the synthesized nanoparticles was calculated using Scherrer's equation:  $D = k\lambda/\beta\cos\theta$ , where, D is the average crystalline size, k the Scherrer constant (0.89),  $\lambda$  the X-ray wavelength used,  $\beta$  the angular line width at half maximum intensity and  $\theta$  is the Bragg's angle in degrees unit.35 The calculated average particle sizes are 13 and 10 nm for CuO and CuOGA-TSCPy, respectively. The XRD pattern obtained for the CuOTSCPy (Figure 2c) is different from those observed for CuO and CuO-GA-TSCPy and is relatively broader. No sharp peaks can be attributed to the amorphous nature of CuOTSCPy powders. In addition, the peaks related to the CuS phase were also identified in Figure 2c. 36 These phenomena can be mainly explained by the presence of TSCPy during the formation of CuO phase in the synthesis of CuOTSCPv nanoparticles. As known, thiocarbamates and thiocarbazides have been used frequently for the synthesis of CuS nanoparticles, <sup>37,38</sup> and this can be one of the disadvantages of direct functionalization of CuO nanoparticles using method B.

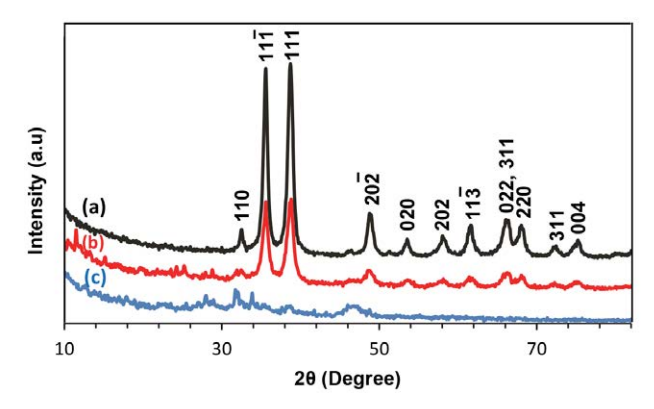


**Figure 2.** The XRD patterns of the synthesized samples of (a) CuO (b) CuOGA-TSCPy and (c) CuOTSCPy nanoparticles.

The morphology and particle size of the synthesized samples were also investigated by scanning electron microscopy (SEM). SEM images show that the nanoparticles have almost spherical shape (Figure 3). The particles are well separated and uniformly distributed. The average particle sizes

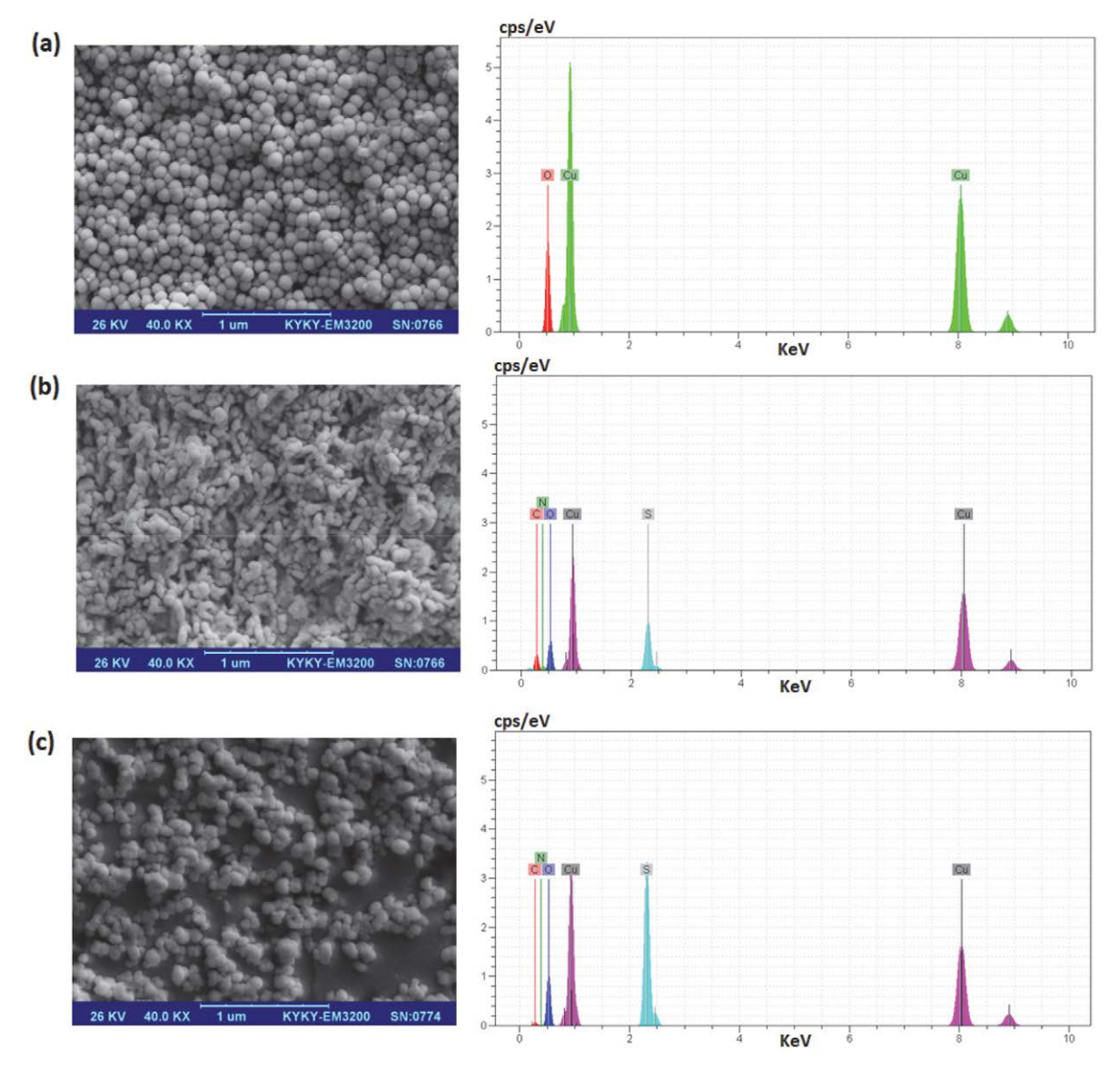


Figure 3. SEM and EDX images of (a) CuO (b) CuOGA-TSCPy (c) CuOTSCPy nanoparticles.

estimated from the SEM images were about 58, 42 and 52 nm for CuO, CuOGA-TSCPy and CuOTSCPy, respectively. The larger size of the functionalized nanoparticles might be due to the capping of nanoparticles by GA and/or TSCPy confirmed by FT–IR analysis. To provide further information about the elemental composition of the prepared nanoparticles, the samples were characterized by energy dispersive X-Ray (EDX) analysis. As shown in Figure 3, results clearly demonstrated the purity of the synthesized CuO, CuOGA-TSCPy and CuOTSCPy nanoparticles.

#### 3. 3. Antibacterial Activity

The antibacterial activities of TSCPy, and also CuO, CuOGA, CuOGA-TSCPy and CuOTSCPy nanoparticles were studied against Gram-positive and Gram-negative bacterial strains including *Micrococcus luteus* (*M. luteus*),

Staphylococcus aureus (S. aureus), Escherichia coli (E. coli) and Pseudomonas aeruginosa (P. aeruginosa), using the zone inhibition method. Penicillin G and tetracycline were used as positive controls. The antibacterial activity of tested agents was monitored at a concentration of 2000 µg/mL in DMSO and the experiments were performed in triplicate. The trend in antimicrobial activity of four compounds was determined by measuring the inhibition zone around the well and the results are presented in Table 1. The data shows that the synthesized compounds are active against almost all the microorganisms under study. TSCPy free ligand showed the highest antibacterial activity among all of the synthesized compounds. Moreover, antibacterial activities of glutamic acid functionalized CuO (CuOGA) and CuO nanoparticle were the same against Gram-positive and Gram-negative bacterial strains. The addition of TSCPY to the structure of CuOGA increased the antibac-

Compounds	zone of inhibition (mean ± SD, mm)				
-	Gram-positive		Gram-	negative	
	M. luteus	S. aureus	E. coli	P. aeruginosa	
TSCPy	53.5 ± 3.5	35.7 ± 4.5	$25.5 \pm 0.5$	27.5 ± 2.5	
CuO	$21.5 \pm 2$	$13.5 \pm 0.5$	$8.5 \pm 0.5$	$16.5 \pm 0.8$	
CuOGA	$21 \pm 1.5$	8	8	$15 \pm 1$	
CuOGA-TSCPy	$28 \pm 1$	$21.5 \pm 2.5$	$12 \pm 1$	$12.5 \pm 1$	
CuOTSCPy	$16 \pm 1.5$	$23 \pm 2$	8	$19.5 \pm 0.5$	
Penicillin G	$50 \pm 1$	$50 \pm 1$	$18 \pm 1$	_	
Tetracycline	$46 \pm 1$	$41 \pm 1$	$31 \pm 1$	$27 \pm 1$	

 Table 1. Antibacterial activity of synthesized compounds and comparison to penicillin and tetracycline.

terial activity of CuOGA-TSCPy against M. luteus ( $28 \pm 1$ ), S. aureus ( $21.5 \pm 2.5$ ) and E. coli ( $12 \pm 1$ ). Furthermore, CuOTSCPy showed higher antibacterial activity in comparison with CuO against S. aureus ( $23 \pm 2$ ) and P. aeruginosa ( $19.5 \pm 0.5$ ). Results in Table 1 confirm that the functionalization of CuO with the bioactive TSCPy moiety can enhance antibacterial activity.

Furthermore, the observed MIC and MBC for the respective microorganisms are shown in Table 2. MIC is the lowest concentration of the antimicrobial agent that inhibits microbial growth and MBC was also determined as the lowest bactericidal concentration of the tested compound. For CuO, it was found that the MIC and the MBC were 10 μg/mL and 20 μg/mL for M. luteus respectively. The best MIC value for TSCPy (10 µg/mL) was found against S. aureus and E. coli, whereas it was more than 25 μg/ml for CuO. MBC was not reached using CuO against S. aureus, E. coli and P. aeruginosa. The behavior of CuOGA-TSPy and CuOTSPy was similar. The results of our studies showed that the CuOGA-TSPy and CuOTSPy nanoparticles not only showed bacteriostatic effects, but also exhibited bactericidal activity in most cases. According to the MBC results, it was found that antimicrobial activity of nano-sized CuO was enhanced after functionalization with the TSCPy moiety (Table 2).

The contribution of the size, shape, morphology, and capping agents on bactericidal effect of metal oxide nanoparticles and their interaction with microbial membranes

have been previously proven.<sup>39-42</sup> Previous studies revealed that CuO nanoparticles prepared by various procedures have shown different physicochemical properties that govern the antibacterial activity (Table 3). The obtained values of zone of inhibition demonstrate that CuO, CuOGA-TSCPy and CuOTSCPy nanoparticles prepared by the described method have higher antibacterial activities compared with previously published values.<sup>43-47</sup> This can be attributed to their size, shape and high surface to volume ratio, and also the synergetic effect of CuO and thiosemicarbazone moieties.

#### 4. Conclusions

Copper oxide nanoparticles were synthesized by sonochemical method and functionalized with the bioactive 2-acetylpyridine thiosemicarbazone molecule through two different methods: **A** and **B** routes, yielding the CuO-GA-TSCPy and CuOTSCPy nanoparticles, respectively. In method **A**, nanoparticles were first functionalized with glutamic acid, followed by a subsequent condensation step between glutamic acid and thiosemicarbazone. In method **B**, the surface of the CuO nanoparticles is directly modified with 2-acetylpyridine thiosemicarbazone. The bactericidal activity of bare CuO and functionalized CuO nanomaterials prepared using **A** and **B** routes was tested *in vitro* using the zone inhibition method against Gram positive

<b>Table 2.</b> MIC and MBC values for synthesized	l compounds against different bacterial strains.
--	--

CompoundsCompound concentration (µg/mL)								
	Gram-positive bacteria				Gram-negative bacteria			
	M. luteus		S. aureus		E. coli		P. aeruginosa	
	MIC	MBC	MIC	MBC	MIC	MBC	MIC	MBC
TSCPy	20	20	10	20	10	20	_	_
CuO	10	20	_	_	20	_	_	_
CuOGA	10	10	_	_	10	10	_	_
CuOGA-TSCPy	2.5	2.5	10		20	20	_	_
CuOTSCPy	5	2.5	10	10	10	_	10	10
Penicillin G	15.6		15.62		62.5		1000	
Tetracycline	31.3		62.5		31.25		15.62	

Table 3. Comparative results for physical properties and antibacterial activity of CuO nanoparticles synthesized with different methods.

Chemical composition	Method of synthesis	Shape	Size (nm)	Microorganism (growth inhibition Ref. hole, mm)		
CuO	green synthesis	spherical	Less than 100	E. coli (12.8); S. aureus (12)	[43]	
CuO	electrochemical reduction	spherical	5–10 nm	E. coli (5); S. aureus (12)	[44]	
CuO	hydrothermal reaction, low temperature sonochemical	nanoflowers, nanoleaves, nanoflakes, nano rod	50–100	S. aureus (nanoflakes: 10 and nanoleaves: 12); S. pneumonia* (nanoflakes: 15, nanoleaves: 12); S. typhimurium** (nanoflakes: 14, nanoleaves: 16)		
CuO and biosynthesis Ag/CuO nanocomposite		spherical	Less than 10	S. pneumonia ( CuO:13 and Ag/CuO: 24 )	[46]	
polyindole/ reflux condensation Ag–CuO nanocomposite		plates like, leaf like, flower buds like	Less than 20	E. coli (5); S. aureus (10)	[47]	
CuO	sono-chemical	spherical	40.4-57.6	S. aureus (13.5); M. luteus (21.5); P. aeruginosa (16.5)	This study	
CuOGA- TSCPy	sono-chemical	spherical	37.8-52.8	S. aureus (21.5); M. luteus (28); P. aeruginosa (12); E. coli (12.5)	This study	
CuOTSCPy	sono-chemical	spherical	49.2-56.3	S. aureus (23); M. luteus (16); P. aeruginosa (19.5)	This study	

<sup>\*</sup> Streptococcus pneumonia \*\* Salmonella typhimurium

and Gram negative bacterial strains. MIC and MBC values were also determined. The CuOTSCPy nanoparticles possess lower crystallinity and phase purity than CuOGA-TSCPy nanoparticles. This might be due to the presence of thiosemicarbazone during the formation of CuO phase leading to formation of some impurities such as CuS. Compared with previously published experimental results, CuO, CuOGA-TSCPy and CuOTSCPy nanoparticles synthesized by the sonochemical method showed higher antibacterial activities. Moreover, antibacterial activity of nano-sized CuO was enhanced after functionalization with thiosemicarbazone moiety.

#### Acknowledgements

The authors are grateful to the University of Guilan for financial support.

#### 5. References

- A. MacGowan, E. Macnaughton, *Medicine* 2013, 41, 642–648.
   DOI:10.1016/j.mpmed.2013.08.002
- Q. Li, S. Mahendra, D. Y. Lyon, L. Brunet, M. V. Liga, D. Li, P.J. Alvarez, Water Res. 2008, 42, 4591–4602.
   DOI:10.1016/j.watres.2008.08.015
- 3. M. A. Elkodous, G. S. El-Sayyad, I. Y. Abdelrahman, H. S. El-Bastawisy, A. E. Mohamed, F. M. Mosallam, H. A. Nasser, M. Gobara, A. Baraka, M. A. Elsayed, A. I. El-Batal, *Colloids Surf. B Biointerfaces* **2019**, *180*, 411–428.

DOI:10.1016/j.colsurfb.2019.05.008

 F. Hossain, O. J. Perales-Perez, S. Hwang, F. Roman, Sci. Total. Environ. 2014, 466, 1047–1059.

**DOI:**10.1016/j.scitotenv.2013.08.009

- N. Beyth, Y. Houri-Haddad, A. Domb, W. Khan, R. Hazan, *Evid. Based Complement. Alternat. Med.* 2015, 2015, Article ID 246012 DOI:10.1155/2015/246012
- V. K. Sharma, R. A. Yngard, Lin Y., Adv. Colloid Interface Sci. 2009, 145, 83–96. DOI:10.1016/j.cis.2008.09.002
- X. Gu, Z. Xu, L. Gu, H. Xu, F. Han, B. Chen, X. Pan, Environ. Chem. Lett. 2021, 19, 167–187.

**DOI:**10.1007/s10311-020-01071-0

- B. Shekoufeh, L. Azhar, F. Lotfipour, *Die Pharmazie-An Int. J. Pharm. Sci.* 2012, 67, 817–821. DOI:10.1002/jccs.201600735
- 9. S. Yadav, G. Jaiswar, J. Chin. Chem. Soc. 2017, 64, 103-116.
- M. Nejati, M. Rostami, H. Mirzaei, M. Rahimi-Nasrabadi, M. Vosoughifar, A. S. Nasab, M. R. Ganjali, *Inorg. Chem. Commun.* 2022, 136, 109107–109139.

DOI:10.1016/j.inoche.2021.109107

 S. Parham, D. H. Wicaksono, S. Bagherbaigi, S. L. Lee, H. Nur, J. Chin. Chem. Soc. 2016, 63, 385–393.

DOI:10.1002/jccs.201500446

- R. Kumar, A. Umar, G. Kumar, H. S. Nalwa, *Ceram. Int.* 2017, 43, 3940–3961. DOI:10.1016/j.ceramint.2016.12.062
- G. Ren, D. Hu, E. W. Cheng, M. A. Vargas-Reus, P. Reip, R. P. Allaker, *Int. J. Antimicrob. Agents* 2009, 33, 587–590.
   DOI:10.1016/j.ijantimicag.2008.12.004
- H. Kumar, R. Rani, Rec. Adv. Biomed. Chem. Eng. Mater. Sci. 2014, 197–200.
- 15. S. Gaysinsky, P. M. Davidson, B. D. Bruce, J. Weiss, J. Food

- Prot. 2005, 68, 1359–1366.
- DOI:10.4315/0362-028X-68.7.1359
- A. Fernández-Agulló, E. Pereira, M. S. Freire, P. Valentao, P. B. Andrade, J. González-Álvarez, J. A. Pereira, *Ind. Crop. Prod.* 2013, 42, 126–132. DOI:10.1016/j.indcrop.2012.05.021
- 17. P. Elena, K. Miri, *Colloids Surf. B Biointerfaces* **2018**, *169*, 195–205. **DOI**:10.1016/j.colsurfb.2018.04.065
- N. Talebian, S. M. Amininezhad, M. Doudi, *J. Photochem. Photobiol. B* 2013, *120*, 66–73.
   DOI:10.1016/j.jphotobiol.2013.01.004
- R. A. Bohara, N. D. Thorat, H. M. Yadav, S. H. Pawar, New J. Chem. 2014, 38, 2979–2986. DOI:10.1039/c4nj00344f
- N. Sampath, R. Mathews, M. N. Ponnuswamy, *J. Chem. Crystallogr.* 2010, 40, 1099–1104.
   DOI:10.1007/s10870-010-9802-y
- T. S. Lobana, R. Sharma, G. Bawa, S. Khanna, Coord. Chem. Rev. 2009, 253, 977-1055. DOI:10.1016/j.ccr.2008.07.004
- 22. J. R. Dilworth, R. Hueting, *Inorg. Chim. Acta* **2012**, *389*, 3–15. **DOI:**10.1016/j.ica.2012.02.019
- 23. Z. Piri, Z. Moradi–Shoeili, A. Assoud, *Inorg. Chim. Acta* **2019**, 484, 338–346. **DOI:**10.1016/j.ica.2018.09.054
- 24. A. S. Ethiraj, D. J. Kang, *Nanoscale Res. Lett.* **2012**, *7*, 70–75. **DOI:**10.1186/1556-276X-7-70
- 25. S. Hosseinpour, F. Tang, F. Wang, R. A. Livingstone, S. J. Schlegel, T. Ohto, M. Bonn, Y. Nagata, E. H. Backus, *J. Phys. Chem. Lett.* **2017**, *8*, 2195–2199.
  - DOI:10.1021/acs.jpclett.7b00564
- A. Azam, A. S. Ahmed, M. Oves, M. S. Khan, A. Memic, *Int. J. Nanomedicine* 2012, 7, 3527–3535.
   DOI:10.1039/C2TA00084A
- B. Zhao, P. Liu, H. Zhuang, Z. Jiao, T. Fang, W. Xu, B. Lu, Y. Jiang, J. Mater. Chem. A 2013, 1, 367–373.
- 28. L. Jin, Y. Wang, *Phys. Chem. Chem. Phys.* **2017**, *19*, 12992–13001. **DOI**:10.1039/C7CP01715D
- D. M. Wiles, T. Suprunchuk, Can. J. Chem. 1969, 47, 1087– 1089. DOI:10.1139/v69-173
- 30. D. M. Wiles, B. A. Gingras, T. Suprunchuk, *Can. J. Chem.* **1967**, *45*, 469–473. **DOI:**10.1139/v67-081
- A. Balaban, M. Şekerci, B. Erk, Synth. React. Inorg. M. 2003, 33, 1775–1786. DOI:10.1081/SIM-120026547

- N. Moorthy, P. J. Prabakar, S. Ramalingam, M. Govindarajan,
   J. Gnanamuthu, G. V. Pandian, *J. Phys. Chem. Solids* 2016,
   74–88. DOI:10.1016/j.jpcs.2016.04.002
- Z. Piri, Z. Moradi-Shoeili, A. Assoud, *Inorg. Chem. Commun.* 2017, 84, 122–126. DOI:10.1016/j.inoche.2017.08.005
- 34. J. Song, L. Xu, C. Zhou, R. Xing, Q. Dai, D. Liu, H. Song, ACS Appl. Mater. Interfaces 2013, 5, 12928–12934. DOI:10.1021/am403508f
- H. P. Kluge, L. E. Alexander, in X-ray Diffraction Procedure, Wiley Inter Science, New York, 1974.
- R. A. Zarate, F. Hevia, S. Fuentes, V. M. Fuenzalida, A. Zuniga, *J. Solid State Chem.* 2007, 180, 1464–1469.
   DOI:10.1016/j.jssc.2007.01.040
- P. A. Ajibade, N. L. Botha, Results in physics 2016, 6, 581–589.
   DOI:10.1016/j.rinp.2016.08.001
- B. Srinivas, B. G. Kumar, K. Muralidharan, *J. Mol. Catal. A-Chem.* 2015, 410, 8–18.
   DOI:10.1016/j.molcata.2015.08.028
- A. Sirelkhatim, S. Mahmud, A. Seeni, N. H. M. Kaus, L. C. Ann, S. K. M. Bakhori, H. Hasan, D. Mohamad, *Nano-Micro Lett.* 2015, 7, 219–242. DOI:10.1007/s40820-015-0040-x
- L. E. Shi, Z. H. Li, W. Zheng, Y. F. Zhao, Y. F. Jin, Z. X. Tang, Food Addit. Contam. Part A 2014, 31, 173–186.
   DOI:10.1080/19440049.2013.865147
- S. Pal, Y. K. Tak, J. M. Song, Appl. Environ. Microbiol. 2007, 73, 1712–1720. DOI:10.1128/AEM.02218-06
- S. Nair, A. Sasidharan, V. D. Rani, D. Menon, S. Nair, K. Manzoor, S. Raina, J. Mater. Sci.: Mater. Med. 2009, 20, 235–242.
   DOI:10.1007/s10856-008-3548-5
- 43. G. Sharmila, M. Thirumarimurugan, V. M. Sivakumar, *Optik* **2016**, *127*, 7822–7828. **DOI**:10.1016/j.ijleo.2016.05.142
- 44. S. Jadhav, S. Gaikwad, M. Nimse, A. Rajbhoj, *J. Clust. Sci.* **2011**, *22*, 121–129. **DOI**:10.1007/s10876-011-0349-7
- S. Sonia, R. Jayasudha, N. D. Jayram, P. S. Kumar, D. Mangalaraj, S. R. Prabagaran, *Curr. Appl. Phys.* **2016**, *16*, 914–921.
   **DOI:**10.1016/j.cap.2016.05.006
- 46. N. Ghasemi, F. Jamali-Sheini, R. Zekavati, *Mater. Lett.* **2017**, *196*, 78–82. **DOI**:10.1016/j.matlet.2017.02.111
- M. Elango, M. Deepa, R. Subramanian, A. M. Musthafa, *Polym. Plast. Technol. Eng.* 2018, 57, 1440–1451.
   DOI:10.1080/03602559.2017.1410832

#### Povzetek

S sonokemijsko metodo smo sintetizirali organsko – anorganske hibridne nanomateriale, pri čemer smo uporabili dva različna pristopa za sidranje 2-acetilpiridin tiosemikabazona na površino nanodelcev CuO. Sintetizirane nanodelce smo karakterizirali s kombinacijo fizikalno-kemijskih in spektroskopskih metod. Sinergijsko baktericidno aktivnost CuO in tiosemikabazona smo testirali *in vitro* proti grampozitivnim in gramnegativnim bakterijam. Določili smo tudi minimalno inhibitorno koncentracijo in minimalno baktericidno koncentracijo. Rezultati kažejo, da nanodelci CuO in funkcionalizirani nanodelci CuO, pripravljeni po sonokemijski metodi iz te raziskave, kažejo izboljšano baktericidno aktivnost in bi lahko bili uporabni v pripravi učinkovitejših antibakterijskih materialov za farmacevtsko uporabo.



Except when otherwise noted, articles in this journal are published under the terms and conditions of the Creative Commons Attribution 4.0 International License